International Journal of Thermal Sciences 50 (2011) 2304–2310

Contents lists available at ScienceDirect

International Journal of Thermal Sciences

journal homepage: www.elsevier.com/locate/ijts

Contribution of an internal heat exchanger to the performance of a liquid desiccant dehumidifier operating near freezing conditions

Sergio M. Pineda, Gerardo Diaz*

School of Engineering, University of California Merced, 5200 North Lake Rd, Merced, CA 95343, USA

ARTICLE INFO

Article history:
Received 1 February 2011
Received in revised form
1 June 2011
Accepted 4 June 2011
Available online 13 July 2011

Keywords:
Liquid desiccants
Internal heat exchangers
Refrigerated warehouse

ABSTRACT

The aim of the present study is to analyze numerically the effect of an internal heat exchanger (IHX) in a liquid-desiccant based dehumidification system operating near freezing conditions that are typical of a refrigerated warehouse. The study is based on previous work done by the authors that showed reduced ice formation on the surface of a cooling coil by dehumidifying the air using liquid desiccants. The results of the present study show that IHX effectiveness has a direct impact on the inlet temperature of the liquid desiccant leaving the absorber. High IHX effectiveness results in high absorber effectiveness. However, IHX effectiveness less than 60% leads to a desorption process where the liquid desiccant concentration increases, augmenting the humidity ratio of the air going through the mass exchanger.

1. Introduction

The growth in the demand for energy has been projected to increase by about 50 percent from 2005 to 2030 [1]. The main source of energy to match this demand will come from fossil fuels that are currently facing increasing uncertainty with respect to their long-term availability. They also play an important role in augmenting the emission of greenhouse gases to the atmosphere [2,3]. A feasible option for matching rising demand without increasing power generation is to improve energy efficiency in residential, commercial, and industrial applications. One example of an energy intensive industrial application is the refrigerated warehouse sector. A refrigerated warehouse operates as a traditional vapor-compression refrigeration cycle. The evaporator is installed inside the cold storage and the compressor and cooling towers are located outside. Agricultural produce is brought in and out of the pre-cooling rooms allowing hot and humid air to enter the cold storage. The quality of the produce is maintained by keeping a high relative humidity inside the room and the temperature remains near freezing conditions. These operating conditions translate into a continuous formation of ice on the surface of the evaporator. Therefore, defrosting cycles are run between one to three times a day to remove the ice from the evaporator. Defrosting cycles are inherently inefficient since they raise the surface temperature of the evaporator and involve the use of natural gas, propane, or water sprays to melt the ice.

Hybrid vapor-compression/liquid-desiccant cooling systems have been analyzed in the past as an alternative that reduces energy consumption in air conditioning and refrigeration applications. Yadav [4] suggested energy savings of up to 80% when the latent load constitutes 90% of the total cooling load with a liquid-desiccant dehumidifier regenerated by solar energy. Pineda and Diaz showed reduced energy and defrosting-water consumption in cold storages where a liquid desiccant absorber was used to remove moisture from the air upstream of the evaporator [5–7].

Although a number of researchers have analyzed dehumidification and cooling systems that utilize liquid desiccants [8–13] the study of liquid desiccant systems operating near freezing conditions has received little attention. A literature review of the theoretical and physical models of a refrigerated warehouse, as well as, the comparisons between a traditional vapor-compression cycle and a liquid desiccant refrigeration cycle are found in [8]. Elsayed et al. [14] analyzed the performance of an air cycle refrigerator combined with a desiccant rotor for an air conditioning application. More recently, the same authors numerically analyzed the performance of an air cycle refrigerator integrated with a desiccant system for cooling and dehumidifying a warehouse [15]. They found that the coefficient of performance (COP) can increase more than one hundred percent with respect to a conventional system. In general, COP improvement in vapor-compression systems using liquid desiccants is shown to depend on three main factors: the type of liquid desiccant used [16,17], the effectiveness of the

* Corresponding author. Tel.: +1 209 228 7858; fax: +1 209 228 4047.
E-mail address: gdiaz@ucmerced.edu (G. Diaz).

1290-0729/$ – see front matter © 2011 Elsevier Masson SAS. All rights reserved.
doi:10.1016/j.ijthermalsci.2011.06.003

Nomenclature

C	water concentration in desiccant ($kg_{H_2O} kg^{-1}_{solution}$)
COP	coefficient of performance
D	diffusivity ($m^2\ s^{-1}$)
h_{gf}	enthalpy of condensation ($J\ kg^{-1}$)
H	absorber height (m)
k	thermal conductivity ($W\ m^{-1}\ K^{-1}$)
L	absorber depth (m)
p_t	total pressure (Pa)
p_v	vapor pressure (Pa)
$\dot{Q}$	heat transfer (W)
T	temperature ($^{\circ}C$)
u	velocity in x direction ($m\ s^{-1}$)
v	velocity in y direction ($m\ s^{-1}$)
x	coordinate in x direction
y	coordinate in y direction
z	coordinate in z direction

Greek letters

α	thermal diffusivity ($m^2\ s^{-1}$)
δ	film thickness (m)
ϵ	effectiveness
μ	dynamic viscosity ($kg\ m^{-1}\ s^{-1}$)
ω	humidity ratio ($kg_{H_2O} kg^{-1}_{da}$)
ρ	density ($kg\ m^{-3}$)

Subscripts

a	moist air
abs	absorber
da	dry air
i	inlet condition
int	interface
IHX	internal heat exchanger
l	liquid domain
ld	liquid desiccant
m	moisture
max	maximum
min	minimum

Superscripts

eq	equilibrium
in	inlet condition
out	outlet condition

dehumidifier and regenerator [8,18], and the effectiveness of the internal heat exchanger [6]. However, the effect of the IHX on the performance of a liquid-desiccant system (LDS) has not been analyzed in depth.

Internal heat exchangers are used in refrigeration and air conditioning systems to assure proper system operation and to improve performance [19,20]. Positive benefits in terms of increased COP have been shown by a number of researchers [21–23]. For instance, Vijayan and Srinivasan [23] found that inclusion of an IHX in a window air conditioning unit increased COP by 5.86% for refrigerant R22 and by 6.30% for R407C. However, an IHX can also have a negative influence on the overall performance of the refrigeration cycle. Navarro et al [19] analyzed a refrigeration cycle with and without an IHX for several working fluids detecting that the pressure drop introduced by this device is of significant importance. In general, the adoption of an IHX depends on thermophysical properties of the working fluid and the inlet temperatures to the compressor and evaporator. Typical applications of IHXs are seen in CO_2 transcritical air conditioning systems and heat pumps [24,25].

This work focuses on the effect of the IHX utilized for thermal preconditioning of the liquid desiccant in order to enhance its absorption capabilities before it enters the absorber. Reduction in liquid-desiccant vapor pressure is obtained by reducing its temperature before entering the absorber and thus, better air dehumidification performance is obtained. The thermophysical properties used in the development of the models have been obtained from current published data on liquid desiccants [26,27].

2. System description

The operation of a liquid desiccant system at a refrigerated warehouse is depicted in Fig. 1, that shows how the processes of absorption and regeneration take place at different locations. A concentrated solution of liquid desiccant is pumped at ambient temperature from the bottom of the reservoir tank to the high-pressure side of the IHX and then to the absorber device. At the absorber, the desiccant falls down the walls as a liquid film that is in contact with cold and humid air flowing across the absorber. The indoor air conditions range between 0 and 4 °C and 80–100% RH [5]. The dehumidified air is sent directly to the cold storage evaporator, reducing the formation of ice at its surface. The cold and diluted liquid desiccant exits the absorber and is driven by gravity through the low-pressure side of the IHX where it exchanges energy with the liquid desiccant stream on the high-pressure side, lowering its temperature and thus, enhancing its absorption capabilities. The liquid desiccant leaving the low-pressure side of the IHX drains to the top of the storage tank. Liquid desiccant is pumped from the top of the storage tank to the regenerator where low-relative-humidity ambient air regenerates the liquid desiccant increasing its concentration [7].

In the system being analyzed, the IHX is used with the objective of lowering the temperature of the liquid desiccant and thus, augmenting its absorption properties before it enters the dehumidification device. Fig. 2 shows the IHX device (A) connected to the input and output of the absorber core (B). The exchange of heat between the high and low-pressure sides of the IHX occurs in counter flow configuration.

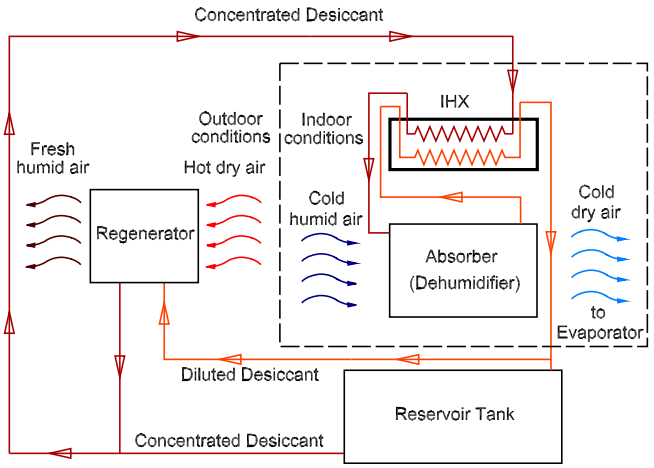

Fig. 1. Absorption–regeneration cycle for the liquid desiccant system operating at a refrigerated warehouse.

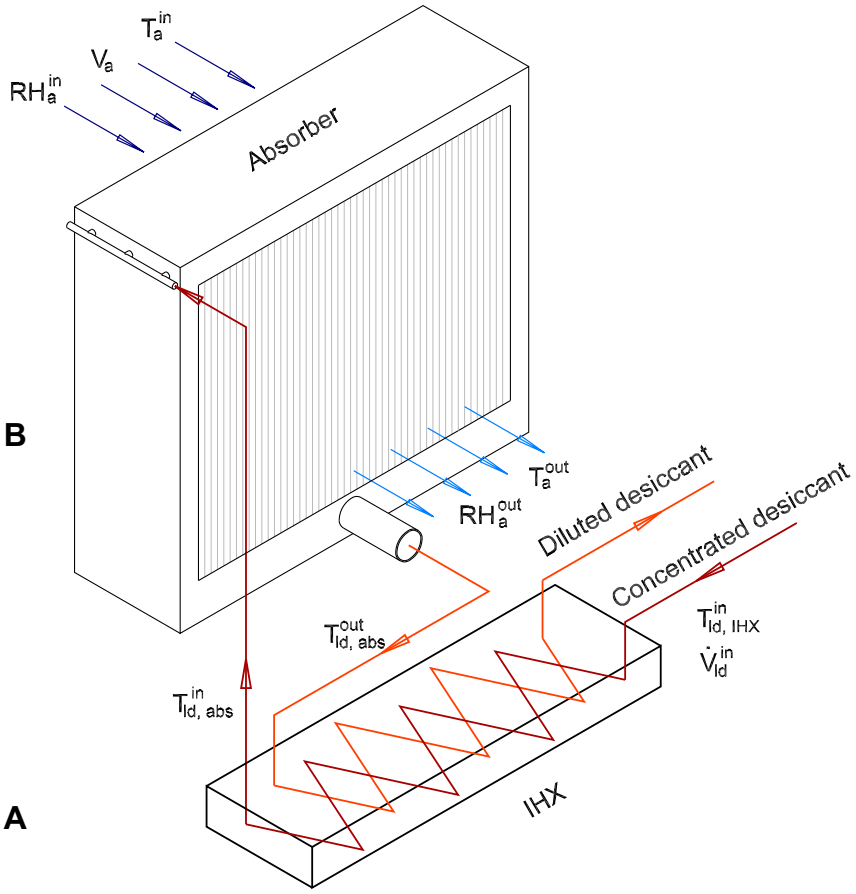

Fig. 2. Schematic of the connections between internal heat exchanger and absorber.

3. Numerical model

In this study a liquid desiccant absorber model, already developed and validated by the authors [5–7,28], is used in combination with a model of an internal heat exchanger to analyze the effect of the IHX on the dehumidifying performance of the absorber core. The setup being studied is shown in Fig. 2. The following assumptions are used in the analysis:

- Laminar flow and fully developed conditions are used.
- Heat losses to the surroundings from the internal heat exchanger are neglected.
- Based on the narrow temperature range studied, constant fluid properties are utilized.
- Steady state conditions are utilized.
- Counter-flow configuration in the internal heat exchanger is considered.
- Negligible thermal resistance at walls and fouling factors.
- The pressure drop in connecting pipelines, hoses, and bends are assumed negligible.

3.1. Absorber

For the dehumidification device, a three-dimensional cross-flow model between a liquid-desiccant film falling on parallel plates and a horizontal humid-air stream was utilized [5,6], where the continuity equation, and equations of motion, energy, and mass transfer are considered in the liquid domain as follows:

$$\frac{\partial v_l}{\partial y_l} = 0, \tag{1}$$

$$\mu_l \frac{\partial^2 v_l}{\partial z_l^2} + \rho_l g = 0, \tag{2}$$

$$v_l \frac{\partial T_l}{\partial y_l} = \alpha_l \frac{\partial^2 T_l}{\partial z_l^2}, \tag{3}$$

$$v_l \frac{\partial C}{\partial y_l} = D_l \frac{\partial^2 C}{\partial z_l^2}, \tag{4}$$

with boundary conditions

$$y_l = 0;\ 0 \le z_l \le \delta_l;\ 0 \le x \le L;\ T_l = T_{l,i};\ C = C_i, \tag{5}$$

$$z_l = 0;\ 0 \le y_l \le H;\ 0 \le x \le L;\ v_l = 0;\ \frac{\partial T_l}{\partial z_l} = 0;\ \frac{\partial C}{\partial z_l} = 0, \tag{6}$$

$$z_l = \delta_l;\ 0 < y_l \le H;\ 0 \le x \le L;\ \frac{\partial v_l}{\partial z_l} = 0;\ T_l = T_a. \tag{7}$$

Similarly, continuity, momentum, energy, and mass transfer equations for the humid-air region are considered as follows:

$$\frac{\partial u_a}{\partial x} = 0, \tag{8}$$

$$\frac{\partial p_a}{\partial x} = \mu_a \frac{\partial^2 u_a}{\partial z_a^2}, \tag{9}$$

$$u_a \frac{\partial T_a}{\partial x} = \alpha_a \frac{\partial^2 T_a}{\partial z_a^2}, \tag{10}$$

$$u_a \frac{\partial \omega}{\partial x} = D_a \frac{\partial^2 \omega}{\partial z_a^2}, \tag{11}$$

with boundary conditions

$$x = 0; 0 \le y_a \le H; 0 \le z_a \le \delta_a; T_a = T_{a,i}; \omega = \omega_i, \tag{12}$$

$$z_a = 0; 0 \le y_a \le H; 0 \le x \le L; \frac{\partial u_a}{\partial z_a} = 0; \frac{\partial T_a}{\partial z_a} = 0; \frac{\partial \omega}{\partial z_a} = 0, \tag{13}$$

$$z_a = \delta_a; 0 \le y_a \le H; 0 \le x \le L; u_a = 0; T_l = T_a; \omega = \omega_{\text{int}}, \tag{14}$$

where ω_{int} and p_v are

$$\omega_{int} = 0.62185 \frac{p_v}{(p_t - p_v)}, \tag{15}$$

$$p_v = p_{v,\mathrm{H_2O}} \left(1 - 0.828(1-C) - 1.496(1-C)^2 + (1-C)\frac{(T_{\text{int}} - 40)}{350}\right) \tag{16}$$

Additionally, energy and mass balances at the liquid – air interface are also considered as follows:

$$-k_l \frac{\partial T_l}{\partial z_l} = k_a \frac{\partial T_a}{\partial z_a} + \rho_a D_a h_{gf} \frac{\partial \omega}{\partial z_a}, \tag{17}$$

$$-\rho_l D_l \frac{\partial C}{\partial z_l} = \rho_a D_a \frac{\partial \omega}{\partial z_a} \tag{18}$$

Finally, the effectiveness of the absorber is defined in Eq. (19),

$$\epsilon_{abs} = \frac{\omega^{in} - \omega^{out}}{\omega^{in} - \omega^{eq}}, \tag{19}$$

where ω^{eq} is the humidity ratio of the air, which is in equilibrium with the desiccant solution at the local solution temperature and concentration [29].

3.2. Internal heat exchanger

The thermal effectiveness of the IHX is calculated as follows:

$$\epsilon_{IHX} = \frac{\dot{Q}}{\dot{Q}_{\max}} = \frac{U_H\left(T_{IHX}^{in} - T_{ld,abs}^{in}\right)}{U_{\min}\left(T_{IHX}^{in} - T_{ld,abs}^{out}\right)}, \tag{20}$$

where $U = \dot{m}c_p$, and T_{IHX}^{in} is the inlet temperature to the high-pressure side of the IHX, $T_{ld,abs}^{in}$ is the outlet of the high-pressure side of the IHX which is the same as the inlet liquid-desiccant temperature to the absorber, and $T_{ld,abs}^{out}$ is the inlet temperature to the low-pressure side of the IHX which is the same as the outlet desiccant solution temperature of the absorber. As fluid properties are considered constant and the mass flow rate on the high and low-pressure side of the IHX are approximately the same, i.e. rate of moisture absorption is small compared to the liquid desiccant flow rate [11,30], then the effectiveness of the internal heat exchanger depends on temperatures only.

Table 1
Operating conditions for the simulations.

Inlet air temperature to absorber	2	°C
Inlet air relative humidity to absorber	90	%
Inlet air velocity to absorber	1.6	m s^{-1}
Inlet liquid desiccant temperature to IHX	20	°C
Mass flow rate of liquid desiccant per unit depth	0.0005	kg m^{-1} s^{-1}
Inlet liquid desiccant concentration	35	%

3.3. Operating conditions for the simulations

The operating conditions used for the heat and mass exchangers have been obtained from measurements at an actual prototype liquid-desiccant system previously analyzed by the authors [5,7]. A typical pre-cooling room that stores produce during a number of hours operates at a range of temperatures between 0 and 4 °C and between 80 and 100% of relative humidity. The values utilized for the input parameters to the model are summarized in Table 1.

Due to availability of experimental test data obtained previously by the authors [7], Calcium Chloride solution was used as liquid desiccant during the simulations. Liquid desiccants absorb moisture from humid air mainly due to the difference in vapor pressure between the air and the desiccant solution. The vapor pressure of a liquid desiccant tends to zero at low temperatures. Thus, absorption capacity is increased by lowering the temperature of the desiccant solution or by increasing its concentration. It is important to operate the liquid desiccant system at conditions where crystallization is not reached. Fig. 3 shows the properties of calcium chloride solution including the change in vapor pressure from 8 to 3.5 mm Hg for calcium chloride solution at 35% concentration for a change in temperature from an inlet value of 20 °C to 4 °C. This process could be obtained utilizing an internal heat exchanger.

4. Results and discussion

The effect of the IHX effectiveness on the absorber outlet air temperature and humidity ratio, and liquid-desiccant

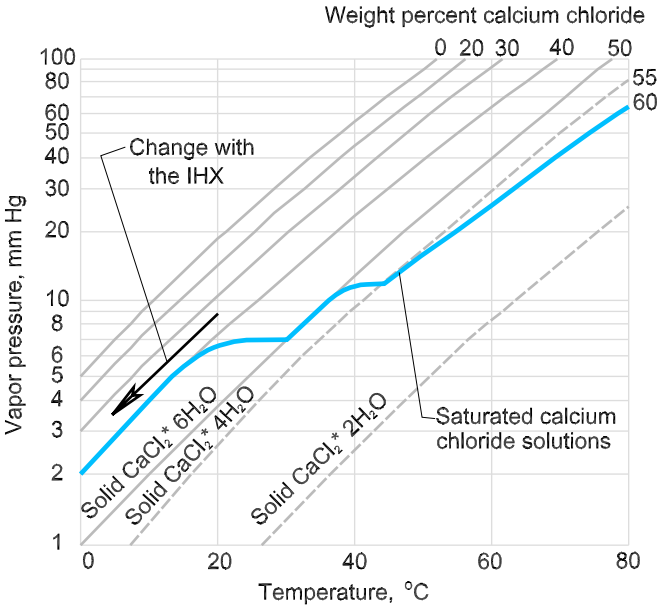

Fig. 3. Vapor pressure change at constant liquid-desiccant concentration due to temperature change. This change in temperature can be obtained using an internal heat exchanger.

Table 2
Inlet simulation conditions: $T_a^{in} = 2\ ^\circ$C, $RH_a^{in} = 90\%$, $C_{ld}^{in} = 35\%$, and $T_{IHX}^{in} = 20\ ^\circ$C.

ϵ_{IHX}[%]	$T_{ld,abs}^{in}$[C]	$\omega_a^{out}[\frac{kg_m}{kg_{da}}]$	T_a^{out}[C]	$T_{ld,abs}^{out}$[C]	C_{ld}^{out}
90	5.8	0.0028	4.3	4.2	32.9
80	8.8	0.0032	6.1	6.0	33.5
70	11.1	0.0035	7.5	7.3	33.9
60	13.1	0.0038	8.7	8.5	34.4
50	14.7	0.0041	9.6	9.4	34.7
40	16.1	0.0043	10.5	10.2	35.1
30	17.3	0.0045	11.2	10.9	35.3
20	18.3	0.0047	11.8	11.5	35.6
10	19.2	0.0049	12.3	12.0	35.8
0	20	0.0051	12.8	12.5	36.0

temperature and concentration is studied first. Considering fixed inlet conditions given by $T_a^{in} = 2\ ^\circ$C, RH = 90%, $C_{ld}^{in} = 35\%$, and $T_{IHX}^{in} = 20\ ^\circ$C, the combined models of the absorber and IHX are utilized to obtain the values of ω_a^{out}, T_a^{out}, $T_{ld,abs}^{out}$, and C_{ld}^{out} based on prescribed values of IHX effectiveness. The results of the simulations are presented in Table 2. The table shows that for a high IHX effectiveness such as $\epsilon_{IHX} = 90\%$ the liquid desiccant temperature entering the absorber, $T_{ld,abs}^{in}$, is reduced from 20 °C to 5.8 °C by the IHX. Thus, at these conditions the humidity ratio of the air is reduced from approximately 0.00392 kg_m/kg_{da} (for $T_a^{in} = 2\ ^\circ$C, $RH_a^{in} = 90\%$) to 0.0028 kg_m/kg_{da}. Moisture from the air is absorbed by the liquid desiccant which lowers its concentration from the initial 35% to 32.9%. The outlet temperatures of air and liquid desiccant at the absorber are 4.3 °C and 4.2 °C, respectively. As the effectiveness of the IHX decreases, $T_{ld,abs}^{in}$ increases and the absorber becomes less effective in dehumidifying the air. The relationship between IHX effectiveness and the inlet liquid desiccant temperature to the absorber is shown in Fig. 4. When ϵIHX is very low, the liquid desiccant enters the absorber near the inlet temperature to the IHX ($T_{IHX}^{in} = 20\ ^\circ$C) and for conditions where $\epsilon IHX \leq 50\%$, the absorber starts acting as a regenerator by increasing the air humidity ratio. This effect is observed in Fig. 5 where the horizontal line denotes the inlet air humidity ratio to the absorber, ω_a^{in}, and the outlet humidity ratio, ω_a^{out}, is represented with diamonds. As the inlet liquid desiccant temperature to the absorber increases, the process changes from air dehumidification to liquid-desiccant regeneration. Outlet humidity ratio

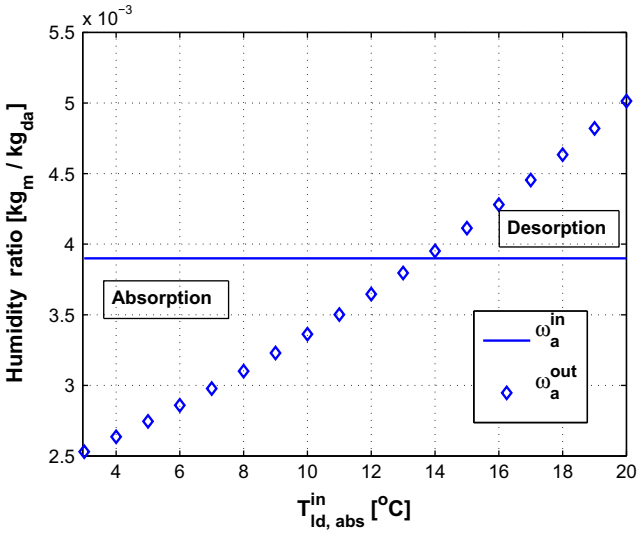

Fig. 5. Outlet air humidity ratio as a function of absorber inlet temperature of the liquid desiccant. The continuous horizontal line represent the inlet humidity ratio and diamonds represent outlet humidity ratio.

versus IHX effectiveness is seen in Fig. 6 where at the simulated operating conditions, the dehumidification process stops near IHX effectiveness of 50% or lower.

As $T_{ld,abs}^{in}$ increases, the absorber becomes less effective in dehumidifying the air and eventually, it starts adding moisture to the air. The outlet liquid desiccant becomes less diluted and the concentration becomes higher than the initial value. Fig. 7 shows this effect, where the inlet liquid concentration, C_{ld}^{in}, is shown as a continuous horizontal line and the outlet liquid-desiccant concentration as circles. It is observed that diluted desiccant with concentration near 32% is obtained at low $T_{ld,abs}^{in}$ which occurs at high IHX effectiveness, but for $T_{ld,abs}^{in} \leq 16\ ^\circ$C the mass exchanger acts as a regenerator increasing the solution concentration with respect to inlet conditions.

Outlet temperatures of air and liquid desiccant are depicted in Fig. 8. As opposed to the slightly nonlinear behavior seen for ω_a^{out} and C_{ld}^{out} with respect to $T_{ld,abs}^{in}$, the outlet air and liquid desiccant

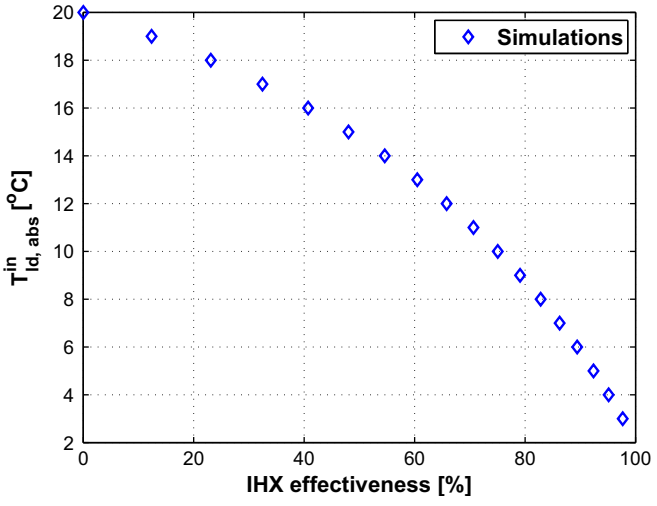

Fig. 4. Inlet liquid desiccant temperature at the absorber as a function of IHX effectiveness. Absorber inlet conditions are: $T_a^{in} = 2^\circ C, RH_a^{in} = 90\%$ and $C_{ld}^{in} = 35\%$.

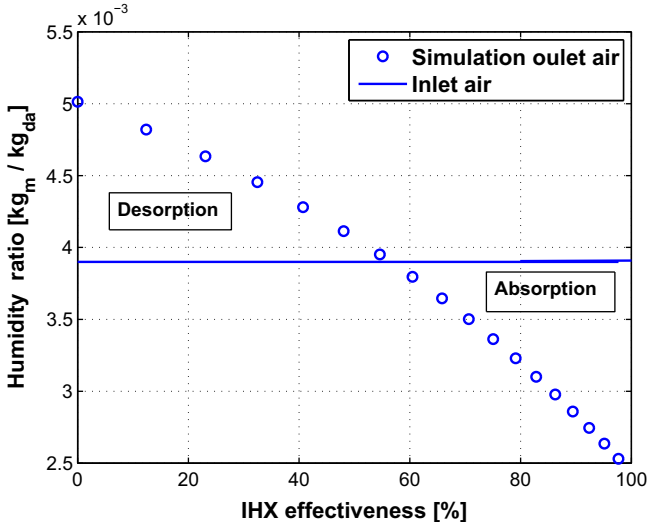

Fig. 6. Outlet humidity ratio versus IHX effectiveness. The continuous horizontal line represent the inlet humidity ratio and circles represent outlet humidity ratio.

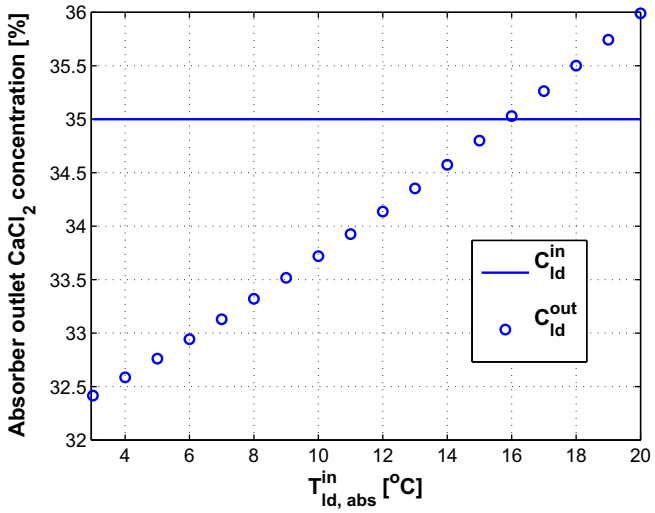

Fig. 7. Outlet calcium chloride concentration versus inlet liquid desiccant temperature at the absorber. The continuous horizontal line represents the inlet solution concentration, circles represent outlet liquid-desiccant concentration.

temperatures, T_a^{out} and $T_{ld,abs}^{out}$, show a linear behavior with a slight divergence as $T_{ld,abs}^{in}$ increases.

The effect of the IHX effectiveness on the outlet conditions of the air going through the absorber are now shown by means of a Psychometric chart in Fig. 9. The arrows in the figure show the dehumidification (or humidification) of the air inside the refrigerated warehouse as a function of IHX effectiveness. It is seen how all the processes end-up at approximately the same outlet relative humidity, i.e. 55%, but with increasing dry-bulb temperatures. However, as the outlet air dry-bulb temperature increases, the initial negative slopes of the process change to positive indicating that the air humidity ratio increases for low ϵIHX. Therefore, it is clear from the figure that a liquid-desiccant based dehumidification system operating inside a refrigerated warehouse with outdoors regeneration, requires an internal heat exchanger in order to remove moisture from the air. If no IHX is used to lower the temperature of the concentrated liquid desiccant solution then the air going through the mass exchanger absorbs moisture instead of rejecting it.

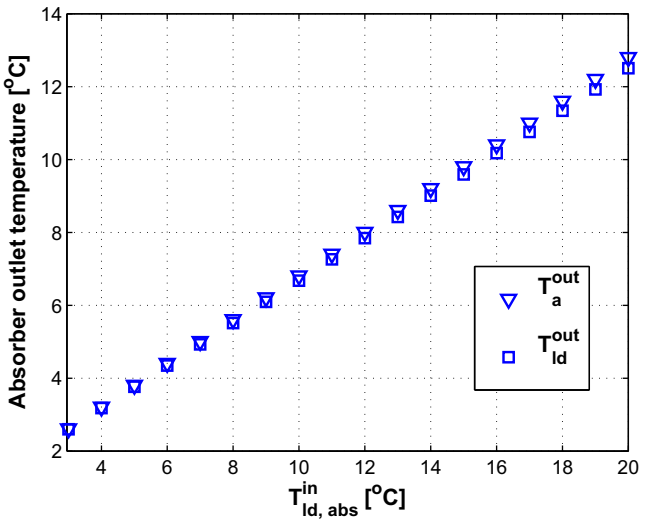

Fig. 8. Outlet temperature for air and liquid desiccant solution versus inlet liquid desiccant temperature at the absorber.

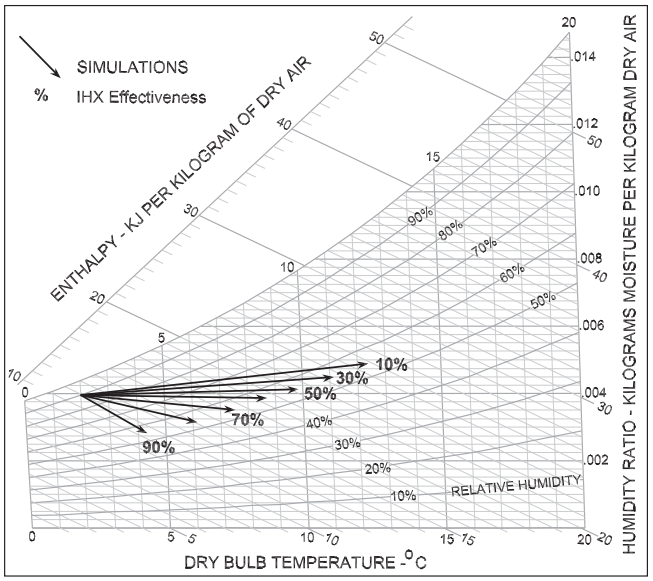

Fig. 9. Absorption-desorption simulations for several IHX effectiveness. Typical absorber inlet conditions are: $T_a^{in} = 2°C, RH_a^{in} = 90\%$ and $C_{ld}^{in} = 35\%$.

Finally, the absorber effectiveness, given by Eq. (19), is plotted as a function of ϵIHX, as seen in Fig. 10. The reference horizontal line at zero absorber effectiveness, ϵ_{abs}, is added to indicate the separation between absorption and desorption behavior of the mass exchanger. It is observed that for the absorption process, a higher IHX effectiveness implies a higher absorber effectiveness. In order to have high absorber effectiveness, i.e. ϵ_{abs}>50%, ϵIHX needs to be higher than 85%, approximately. The curve is extended to negative values of ϵ_{abs} only to show the desorption process when ϵIHX is low. The dehumidification system is not intended to operate under such conditions.

The findings obtained in this study indicate that under the operating conditions simulated, an internal heat exchanger is indeed required to dehumidify the air inside a refrigerated warehouse with a liquid desiccant solution. Moreover, the effectiveness of the IHX needs to be higher than 60%, otherwise desorption occurs.

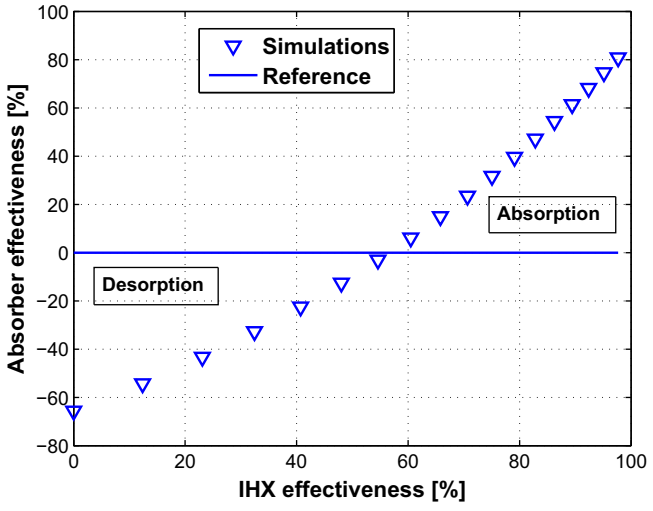

Fig. 10. Absorber effectiveness versus IHX effectiveness. Absorption and desorption regions are depicted as a function of several IHX effectiveness and for the following absorber inlet conditions: $T_a^{in} = 2°C, RH_a^{in} = 90\%$ and $C_{ld}^{in} = 35\%$.

5. Conclusions

The effect on liquid desiccant absorber performance operating near freezing conditions as a function of internal heat exchanger effectiveness is studied numerically. An internal heat exchanger effectiveness model in combination with a previously validated model of a cross-flow absorber with liquid desiccant falling as a film through parallel plates in contact with humid air are used for the simulations. The operating conditions utilized to run the simulations are typical of a cold storage. The results show a strong dependency of the absorber performance with respect to IHX effectiveness. Values of ϵ_{IHX} greater than 60% are required to dehumidify the air. Low IHX effectiveness results in increased humidity ratio of the air going through the mass exchanger. The results also show a significant effect of ϵ_{IHX} in the liquid desiccant temperature at the outlet of the absorber.

Acknowledgment

This work was supported by the California Energy Commission and the California Institute for Energy and Environment contract # MR-07-04.

References

[1] Energy Information Administration, International Energy Outlook 2008-Highlights, Tech. Rep. DOE/EIA-0484. Energy Information Administration, June 2008.
[2] Pacific Gas and Electric Company, Refrigerated Warehouses CASE Report, California Energy Commission Title 24 Buildings Energy Effuciency Standards. Pacific Gas and Electric Company, 2007.
[3] California Energy Commission, Aggregated Data for Investor-owned Utilities, Publicly Owned Utilities, and Combined Utilities. Appendix C, Tech. Rep. California Energy Commission, 2007.
[4] Y.K. Yadav, Vapour compression and liquid-desiccant hybrid solar space - conditioning system for energy conservation, Renewable Energy 6 (7) (1995) 719–723.
[5] S.M. Pineda, Analytical and experimental study of a liquid desiccant heat and mass exchanger operating near water freezing temperature, Master's thesis, Mechanical Engineering, University of California, Merced (April 2009).
[6] S. M. Pineda, G. Diaz, Analysis of heat and mass transfer of an adiabatic cross-flow liquid desiccant absorber operating at low temperatures, in: Proceedings of ASME Summer Heat Transfer Conference, Paper HT2009-88255, San Francisco, 2009, pp. 1–9.
[7] S.M. Pineda, G. Diaz, Performance of an adiabatic cross-flow liquid-desiccant absorber inside a refrigerated warehouse, International Journal of Refrigeration 34 (2011) 138–147.
[8] K. Daou, R. Wang, Z. Xia, Desiccant cooling air conditioning: a review, Renewable and Sustainable Energy Reviews 10 (2006) 55–77.
[9] S. Jain, P. Bansal, Performance analysis of liquid desiccant dehumidification systems, International Journal of Refrigeration 30 (2007) 861–872.
[10] A. Ali, K. Vafai, A. Khaled, Analysis of heat and mass transfer between air and falling film in a cross flow configuration, International Journal of Heat and Mass Transfer 47 (2004) 743–755.
[11] M.S. Park, J.R. Howell, G.C. Vliet, J.L. Peterson, Numerical and experimental results for coupled heat and mass transfer between a desiccant film and air in cross-flow, International Journal of Heat and Mass Transfer 37 (1994) 395–402.
[12] M.S. Park, J.R. Howell, G.C. Vliet, J.L. Peterson, Coupled heat and mass transfer between a falling desiccant film and air in cross flow: Part I - Numerical model and experimental results, AIAA/ASME Heat Transfer Conf. Colorado Springs 275 (1994) 81–90.
[13] M.S. Park, G.C. Vliet, J.R. Howell, Coupled heat and mass transfer between a falling desiccant film and air in cross flow: Part II - Parametric analysis and results, AIAA/ASME Heat Transfer Conf. Colorado Springs 275 (1994) 73–79.
[14] S. Elsayed, Y. Hamamoto, A. Akisawa, T. Ksahiwagi, Analysis of an air cycle refrigerator driving air conditioning system integrated desiccant system, International Journal of Refrigeration 29 (2006) 219–228.
[15] S. Elsayed, T. Miyazaki, Y. Hamamoto, A. Akisawa, T. Ksahiwagi, Performance analysis of air cycle refrigerator integrated desiccant system for cooling and dehumidifying warehouse, International Journal of Refrigeration 31 (2008) 189–196.
[16] X. Liu, Y. Jiang, J. Xia, X. Chang, Analytical solutions of coupled heat and mass transfer processes in liquid desiccant air dehumidifier/regenerator, Energy Conservatins and Management 48 (2007) 2221–2232.
[17] C.Q. Ren, M. Tu, H.H. Wang, An analytical model for heat and mass transfer processes in internally cooled or heated liquid desiccant air contact units, International Journal of Heat and Mass Transfer 50 (2007) 3545–3555.
[18] S. Feyka, V. Kambiz, An investigation of a falling film desiccant dehumidification/regeneration cooling system, Heat Transfer Engineering 28 (2) (2007) 163–172.
[19] J. Navarro-Esbri, R. Cabello, E. Torrella, Experimental evaluation of the internal heat exchanger influence on a vapour compression plant energy efficiency working with R22, R134a, and R407C, Energy 30 (2010) 621–636.
[20] M. Nakagawa, A.R. Marasigan, T. Matsukawa, Experimental analysis on the effect of internal heat exchanger in transcritical CO_2 refrigeration cycle with two-phase ejector, International Journal of Refrigeration (2010) 1–10. doi:10.1016/j.ijrefrig.2010.03.007.
[21] D. Boewe, C. Bullard, J. Yin, P. Hrnjak, Contribution of internal heat exchanger to transcritical R-744 cycle performance, HVAC&R Research 7 (2) (2001) 155–168.
[22] S.G. Kim, Y.J. Kim, G. Lee, M.S. Kim, The performance of a transcritical CO_2 cycle with an internal heat exchanger for hot water heating, International Journal of Refrigeration 28 (2005) 1064–1072.
[23] R. Vijayan, P. Srinivasan, Influence of internal heat exchanger on performance of window AC retrofitted with R407C, Journal of Scientific and Industrial Research 68 (2009) 153–156.
[24] C. Aprea, A. Maiorino, An experimental evaluation of the transcritical CO_2 refrigerator performances using an internal heat exchanger, International Journal of Refrigeration 31 (2008) 1006–1011.
[25] J. Sarkar, Review on cycle modifications of transcritical CO2 refrigeration and heat pump systems, Journal of Advanced Research in Mechanical Engineering 1 (2010) 22–29.
[26] M.R. Conde, Aqueous Solutions Of Lithium And Calcium Chlorides: Property Formulations For Use In Air Conditioning Equipment Design. M. Conde Engineering, Zurich, Switzerland, 2004.
[27] M.R. Conde, Properties of aqueous solutions of lithium and calcium chlorides: formulations for use in air conditioning equipment design, International Journal of Thermal Sciences 43 (4) (2004) 367–382.
[28] G. Diaz, Numerical investigation of transient heat and mass transfer in a parallel-flow liquid-desiccant absorber, Heat and Mass Transfer 46 (2010) 1335–1344.
[29] N. Fumo, D.Y. Goswami, Study of an aqueous lithium chloride desiccant system: air dehumidification and desiccant regeneration, Solar Energy 72 (4) (2002) 351–361.
[30] D. Stevens, J. Braun, S. Klein, An effectiveness model of liquid-desiccant system heat/mass exchangers, Solar Energy 42 (6) (1989) 449–455.